

NASA TECHNICAL NOTE



NASA TN D-5737

C.1

NASA TN D-5737

TECH LIBRARY KAFB, NM
0132329

LOAN COPY: RETURN TO
AFWL (WLOL)
KIRTLAND AFB, N MEX

ESTIMATION OF SPATIAL CAPTURE DISTRIBUTIONS IN RESONANCE ABSORBERS

by Donald Bogart
Lewis Research Center
Cleveland, Ohio



0132329

1. Report No. NASA TN D-5737	2. Government Accession No.	3. Recipient's Catalog No.	
4. Title and Subtitle ESTIMATION OF SPATIAL CAPTURE DISTRIBUTIONS IN RESONANCE ABSORBERS		5. Report Date April 1970	
		6. Performing Organization Code	
7. Author(s) Donald Bogart		8. Performing Organization Report No. E-5186	
9. Performing Organization Name and Address Lewis Research Center National Aeronautics and Space Administration Cleveland, Ohio 44135		10. Work Unit No. 124-09	
		11. Contract or Grant No.	
12. Sponsoring Agency Name and Address National Aeronautics and Space Administration Washington, D. C. 20546		13. Type of Report and Period Covered Technical Note	
		14. Sponsoring Agency Code	
15. Supplementary Notes			
16. Abstract <p>A method is presented for computing spatial distributions of neutron capture in thick layers of resonance absorbers immersed in moderating media. It employs group effective resonance integrals to precalculate group effective resonance cross sections that are universal functions of distance into the absorptive layer. The method is illustrated for captures in uranium-238 for the energy region 0.5 eV to 100 keV. The method is applied to a spherical reactor-shield containing alternate layers of uranium and lithium hydride; large differences in spatial capture and therefore in gamma ray escape fractions are obtained compared to broad multigroup results. Application of the method to the epi-cadmium capture rates at various radii of uranium rods as measured by Hellstrand provided results that agreed with the experiments very well.</p>			
17. Key Words (Suggested by Author(s)) Resonance spatial capture Capture gamma distribution Space reactor shields Spatial uranium burnup Uranium resonance integrals		18. Distribution Statement Unclassified - unlimited	
19. Security Classif. (of this report) Unclassified	20. Security Classif. (of this page) Unclassified	21. No. of Pages 21	22. Price* \$3.00

*For sale by the Clearinghouse for Federal Scientific and Technical Information
Springfield, Virginia 22151

ESTIMATION OF SPATIAL CAPTURE DISTRIBUTIONS IN RESONANCE ABSORBERS

by Donald Bogart
Lewis Research Center

SUMMARY

The problem of precise calculation of spatial distributions of capture in resonance absorbers is crucial to the design of layered shields. Errors in spatial distribution of capture occur in multigroup neutron transport calculations because of the necessarily broad energy groups employed. The single average capture cross section in each group results in large underestimates of the capture rates near surfaces of resonance absorbers. Consequently, the spatial capture gamma ray generation and escape fraction are also in error.

A method is presented for computing spatial resonance capture rates in thick layers. It employs group effective resonance integrals to precalculate group effective resonance cross sections that are universal functions of distance into the absorptive layer. The method is illustrated for captures in uranium-238 for the energy region 0.5 eV to 100 keV.

The method is applied to a spherical reactor-shield configuration that contains alternate layers of depleted uranium and lithium hydride. Detailed comparison is made of the results of a discrete ordinates multigroup calculation with those of the present method. The comparison shows that the difference in spatial capture distribution of the S_n broad treatment of resonance capture causes the capture gamma ray dose to be always underestimated. For example, the difference in spatial capture distribution in a 7-centimeter slab of uranium-238 causes the leakage dose to be a factor of 2 smaller than that obtained with the present method. The apparent generality of the present method suggests that it may be applied directly to the results of layered shield calculations made by S_n broad group methods.

Application of the method to the experimental variation of epi-cadmium capture with depth from the surface of metallic uranium rods up to 5 centimeters in diameter as measured by Hellstrand provided spatial capture rates that agreed with the experiments very well.

INTRODUCTION

The problem of calculating the spatial distributions of capture in resonance absorbers has not been given much attention because in the past only integral capture rates were of primary importance for reactor design. However, in the conceptual design of shields for space power systems, the spatial distributions of capture gamma rays generated in metal layers play a crucial part in the shielding problem.

Some attempts have been made to calculate spatial distributions of captures in resonance absorbers. For uranium rods the problem was approached by Richtmyer (ref. 1) as an illustration of the application of Monte Carlo methods. A spherical harmonics calculation of the radial distribution of neutron capture in a natural uranium rod in the NRX reactor was made by Kushneriuk (ref. 2) for the purpose of understanding the reactivity changes in fuel rods.

The objective of the shielding calculation for a space reactor power source is to solve for the best arrangement of a heavy metal layered within a hydrogenous neutron attenuating material such that a given dose constraint is satisfied with a minimum shield weight. Metals such as tungsten and depleted uranium are considered to be advantageous even though resonance capture generates a considerable secondary gamma ray dose.

Present shield design studies are made using multigroup neutron transport calculations, but the question arises of how to handle the resonance region for thick layers of resonance absorbers. Because of digital computer memory storage limitations the calculations must be made with broad neutron energy groups each encompassing many resonances. In a recent study Lahti (ref. 3) evaluated multigroup and single broad group calculations of captures rates in a slab of depleted uranium. He investigated the 3 to 11 eV neutron range that includes the large resonance at 6.67 eV, using the GAROL code (ref. 4) to evaluate group average cross sections. He found that the broad group failed to represent the multigroup spatial distribution, although the total capture rate was preserved. Therefore, the broad group calculation results in errors in the magnitude of the capture gamma rays that escape from the uranium slab.

The object of this report is to present a method for the accurate estimation of spatial capture distributions in resonance absorbers. The method is illustrated for slabs of uranium-238 for six neutron energy groups covering the range from 0.5 eV to 100 keV.

The method is applied to a spherical reactor-shield configuration that contains alternate layers of depleted uranium and lithium hydride. Detailed comparison is made of spatial capture distributions from a discrete ordinates multigroup calculation with spatial capture distributions obtained by the present method. These comparisons illustrate the effects of broad neutron grouping and the magnitude of resulting differences in capture gamma ray leakage due to incorrect calculation of spatial distribution of captures.

The method is also applied to the experiments of Hellstrand (ref. 5) who measured the variation of epi-cadmium capture with depth from the surface of metallic uranium rods up to 5 centimeters in diameter.

METHODS

The procedure used here applies the results of integral resonance capture theory to estimate spatial distributions of captures within an absorber. Since the absorber will generally be surrounded by moderator regions with slowing down densities of different magnitudes, the procedure will permit the estimation of the spatial distribution for a resonance absorber region in a nonuniform flux environment.

Effective resonance integral. - The effective resonance integral I_{eff} is defined as that lethargy integrated absorption cross section per atom of absorber that will provide the correct capture rate C in an absorber of atom density N and volume V :

$$C = NVI_{\text{eff}}\varphi \quad (1)$$

The flux φ is the scalar flux that exists in the moderating region prior to the insertion of the absorber. It is implicit in equation (1) that for nonabsorptive moderators, the flux varies inversely with neutron energy E . In order for equation (1) to be used quantitatively for a wide range of absorber size and geometry, the quantity I_{eff} must be calculated with precision. The many approaches to the problem of calculating I_{eff} are summarized by Weinberg and Wigner (ref. 6), Dresner (ref. 7), and by Nordheim (ref. 8). It is the method of Nordheim, programmed for digital computer by Kuncir (ref. 9), and extended by Stevens (ref. 4) that obtains direct numerical solutions for the average fluxes in a resonance absorber surrounded by a moderator. The unresolved s-wave resonances are treated by the TUZ code of Kuncir.

In the Nordheim method the average fluxes in the two adjacent media are obtained by solving the coupled integral equations for energy dependent fluxes that express the neutron balance in each region. The spatial transfers of neutrons between the adjacent media are effected by means of their respective collision escape probabilities and application of a reciprocity condition. A space-independent source is assumed in each region for the calculation of these collision escape probabilities for spherical, cylindrical, and slab geometries.

Remarkable success has been achieved in analytical confirmation of experimental values of I_{eff} for many isotopes and absorbers of various geometry (see refs. 6 to 8). For a given isotope of various geometry, values of I_{eff} have been correlated by a surface-to-mass parameter S/M , and it has become conventional to report effective resonance integrals as a function of this parameter. Dresner (ref. 7) has shown that

the average escape probabilities, that are required in the calculation of I_{eff} , are very nearly the same for infinite cylinders, slabs, and spheres when compared on the non-dimensional basis of the ratio of mean chord length \bar{l} to potential scattering mean free paths. The value of \bar{l} is given by $4V/S$ where V/S is the representative volume to surface ratio for the absorber. Therefore, the correlation of measured and calculated values of I_{eff} for a variety of shapes using the surface-to-mass parameter S/M is a reasonable expectation. It is this correlation that is the basis for assuming that the present method that is evolved for slabs, may also be applied to other geometries.

Effective resonance cross section. - The present method for estimating spatial distribution of captures is derived for the case of a slab of thickness t that is infinite in the other directions. The slab is sufficiently thick so as to separate the moderating regions on both sides which in general support different slowing down densities and therefore fluxes of different magnitude. However, for the slab in a symmetrical flux, we make use of the fact that half of the captures are due to the flux in the left region and half due to the flux in the right region. For the unsymmetrical case it is reasonable to expect the captures to divide in proportion to these surface region fluxes and to be independent of each other. Therefore, equation (1) may be written as the sum of the left and right capture rates per unit surface area:

$$C = C_L + C_R = NtI_{\text{eff}}\left(\frac{\varphi_L}{2} + \frac{\varphi_R}{2}\right) \quad (2)$$

where for the slab in a uniform flux, φ_L and φ_R are the equal scalar fluxes in the left and right moderating regions.

Separating the left and right capture rates per unit surface area gives

$$C_L = \frac{NtI_{\text{eff}}}{2} \varphi_L \quad (3)$$

The value of the product $tI_{\text{eff}}/2$ as a function of slab thickness is proportional to the capture rate C_L in the slab surrounded by a $1/E$ slowing down flux. The product approaches zero as t approaches zero and I_{eff} assumes its maximum value of the dilute resonance integral. The product monotonically increases as t gets larger and I_{eff} assumes smaller and smaller values.

A new function, which varies uniquely with distance x from the surface of the slab is defined in the next equation in which the left capture rates are differentiated with respect to x :

$$\frac{dC_L}{dx} = N\phi_L \frac{d\left(\frac{tI_{\text{eff}}}{2}\right)}{dt} \equiv N\phi_L \sigma_{\text{eff}}(x) \quad (4)$$

Equation (4) defines a spatially dependent effective resonance cross section $\sigma_{\text{eff}}(x)$ that is a function of distance x from the left surface and expresses the change in slab capture rate with increment in slab thickness due to the scalar flux in the moderating region on the left. The variation of $\sigma_{\text{eff}}(x)$ with distance x is obtained by numerical differentiation using calculated values of I_{eff} . The variation of $\sigma_{\text{eff}}(x)$ with x varies from one-half the dilute resonance integral at the surface and falls rapidly with distance into the absorber.

For the general case of a slab with different fluxes existing at its face, the total captures per unit surface area due to the specific fluxes in the left and right surface regions are then summed using the generalized values of $\sigma_{\text{eff}}(x)$:

$$C = \int_0^t N\phi_L \sigma_{\text{eff}}(x) dx + \int_0^t N\phi_R \sigma_{\text{eff}}(t - x) dx \quad (5)$$

EFFECTIVE RESONANCE INTEGRALS AND CROSS SECTIONS FOR URANIUM-238

For general use, values of I_{eff} and σ_{eff} have been calculated for uranium-238. The resonance region above 0.5 eV has been divided in the resolved region to 2 keV into five groups with one additional group for the unresolved region extending to 100 keV. A number of groups are required to take care of moderators with a slowing down flux which varies in a manner other than $1/E$. In general, a non- $1/E$ slowing down flux is present in a hydrogenous shielding material such as lithium hydride. It is implicit in any multigroup calculation that a $1/E$ flux exists within each neutron energy group.

The GAROL code (ref. 4) has been used to evaluate effective resonance integrals for the resolved region using the recommended resonance parameters (ref. 10) for uranium-238. Calculations were made for a wide range of slab thicknesses immersed in an infinite sea of hydrogenous moderator. For the unresolved region from 2 to 100 keV the s-wave contributions were calculated using average s-wave resonance parameters determined from the resolved region and the code TUZ (ref. 9). Contributions to

TABLE I. - EFFECTIVE RESONANCE INTEGRALS FOR METALLIC URANIUM-238

Slab thick- ness or rod radius, cm	Geometry parameter, (S/M) ^{1/2}	Neutron energy group						
		0.5 - 10 eV	10 - 25 eV	25 - 100 eV	100 - 500 eV	0.5 - 2 keV	2 - 100 keV	0.5 eV - 100 keV
		Effective resonance integral, I _{eff} , b						
1×10 ⁻⁶	325.0	133.65	59.84	55.31	17.40	3.59	2.78	272.57
1×10 ⁻⁵	102.8	132.77	59.44	54.95	17.36	3.59	2.78	270.89
1×10 ⁻⁴	32.50	127.09	56.87	52.56	17.08	3.59	2.78	259.97
5×10 ⁻⁴	14.54	111.83	49.98	46.25	16.26	3.56	2.77	230.65
.001	10.28	99.36	44.34	41.14	15.48	3.52	2.76	206.60
.005	4.595	57.29	25.28	24.47	12.04	3.32	2.75	125.15
.01	3.250	39.77	17.39	17.71	9.82	3.13	2.74	90.56
.05	1.454	16.10	6.81	8.00	4.92	2.41	2.65	40.89
.1	1.028	11.24	4.66	5.79	3.58	1.98	2.54	29.79
.5	.4595	5.25	2.04	2.87	1.86	1.10	2.22	15.34
1.0	.3250	3.86	1.44	2.15	1.45	.87	2.06	11.83
2.0	.2300	2.85	1.02	1.61	1.15	.71	1.92	9.26
5.0	.1454	1.88	.63	1.07	.90	.56	1.75	6.79
7.0	.1230	1.60	.53	.90	.77	.51	1.68	5.99
10.0	.1028	1.33	.44	.73	.67	.47	1.61	5.25
15.0	.0840	1.06	.36	.55	.57	.41	1.52	4.47
20.0	.0727	.89	.32	.46	.50	.38	1.45	4.00

the dilute resonance integral due to resonances other than s-wave were obtained by lethargy integration of the recommended total capture cross section curve (ref. 10).

Values of I_{eff} are listed in table I and are shown in figure 1 as a function of the geometry parameter $(S/M)^{1/2}$. The dilute or unself-shielded integrals are approached for thin samples on the right and highly self-shielded slabs up to 20 centimeters thick are on the left. Such thick slabs are of interest to the shield designer and it should be noted that all resonance groups are important in the thick region.

Numerical differentiation of each of these curves according to equation (4) provides the variation of the effective resonance cross section $\sigma_{\text{eff}}(x)$ with the distance x from a surface of the slab. These results are listed in table II and are shown in figure 2 for each neutron group. Values of $\sigma_{\text{eff}}(x)$ vary from one-half the dilute resonance integral at the surface to highly self-shielded values deep within a slab. Physically $\sigma_{\text{eff}}(x)$ expresses the change in slab capture rate with increment in slab thickness due to the $1/E$ slowing down flux in the moderating region at one of its surfaces. The rapid reduction of $\sigma_{\text{eff}}(x)$ in the first few thousandths of a centimeter is due to the depletion of the available flux at the resonance peaks; further reduction near the surface is caused by flux depletion in the wings of resonances. The more gradual reduction of $\sigma_{\text{eff}}(x)$ over the

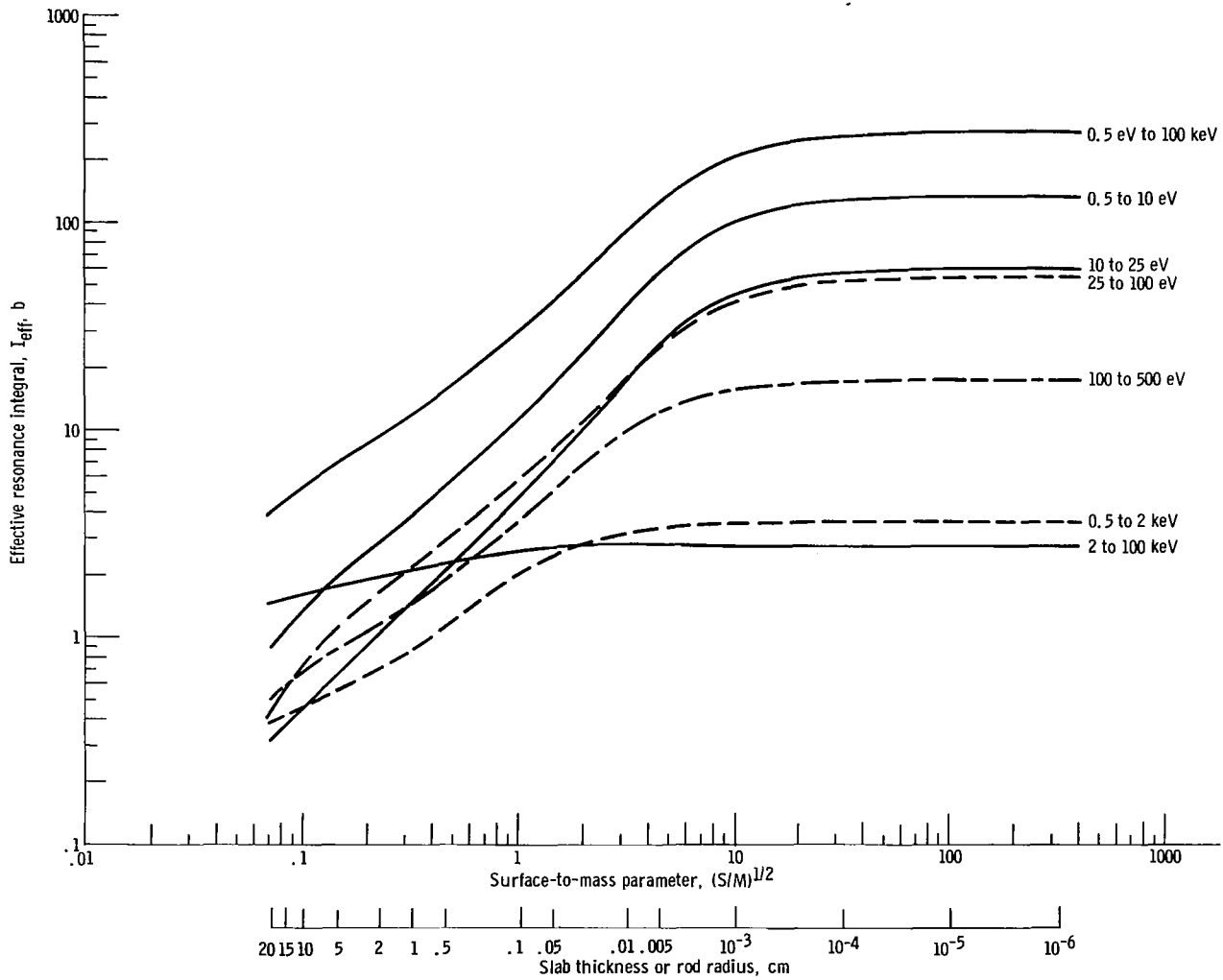


Figure 1. - Group effective resonance integrals for metallic uranium-238.

TABLE II. - EFFECTIVE RESONANCE CROSS SECTIONS FOR
METALLIC URANIUM-238

Distance from sur- face, x, cm	Neutron energy group						
	0.5 - 10	10 - 25	25 - 100	100 - 500	0.5 - 2	2 - 100	0.5 eV -
	eV	eV	eV	eV	keV	keV	100 keV
	Effective resonance cross section, $\sigma_{\text{eff}}(x)$, b						
1×10^{-6}	66.8	29.9	27.7	8.70	1.80	1.40	136.3
1×10^{-5}	66.0	29.5	27.4	8.65	1.79	1.39	134.7
2	65.0	29.2	27.0	8.60			133.0
4	64.5	28.7	26.8	8.55			131.7
6	63.5	28.2	26.4	8.50			129.8
8	62.0	27.7	26.0	8.45			127.3
1×10^{-4}	60.8	27.2	25.5	8.40			125.1
2	56.1	25.5	23.7	8.20	1.78		116.7
4	50.0	22.7	21.0	7.80	1.77	1.38	104.7
6	45.9	20.6	18.9	7.50	1.76		96.0
8	42.6	19.0	17.4	7.25	1.75		89.4
1×10^{-3}	39.6	18.0	16.2	7.05	1.72		84.0
2	28.2	12.4	12.4	6.20	1.67		62.3
4	17.5	8.00	8.60	5.10	1.59	1.37	42.2
6	13.0	5.90	6.35	4.35	1.52	1.37	32.5
8	10.7	4.70	5.10	3.78	1.45	1.36	27.1
1×10^{-2}	9.20	3.90	4.40	3.35	1.40	1.35	23.6
2	6.05	2.45	3.20	2.12	1.23	1.34	16.4
4	4.27	1.63	2.38	1.44	1.00	1.29	12.0
6	3.54	1.32	2.01	1.20	.855	1.25	10.18
8	3.10	1.15	1.77	1.06	.755	1.22	9.06
.1	2.82	1.03	1.62	.970	.680	1.19	8.31
.2	2.13	.760	1.21	.760	.483	1.11	6.45
.4	1.63	.575	.920	.610	.375	1.03	5.14
.6	1.39	.480	.785	.550	.337	.980	4.52
.8	1.23	.417	.700	.510	.315	.950	4.12
1.0	1.11	.372	.630	.483	.300	.930	3.83
2.0	.815	.255	.460	.410	.263	.860	3.06
4.0	.570	.178	.305	.330	.222	.800	2.40
6.0	.453	.147	.235	.275	.200	.760	2.07
8.0	.380	.129	.190	.240	.183	.730	1.85
10.0	.332	.118	.160	.210	.171	.700	1.69
15.0	.252	.102	.115	.165	.150	.650	1.43
20.0	.205	.093	.095	.140	.135	.610	1.28

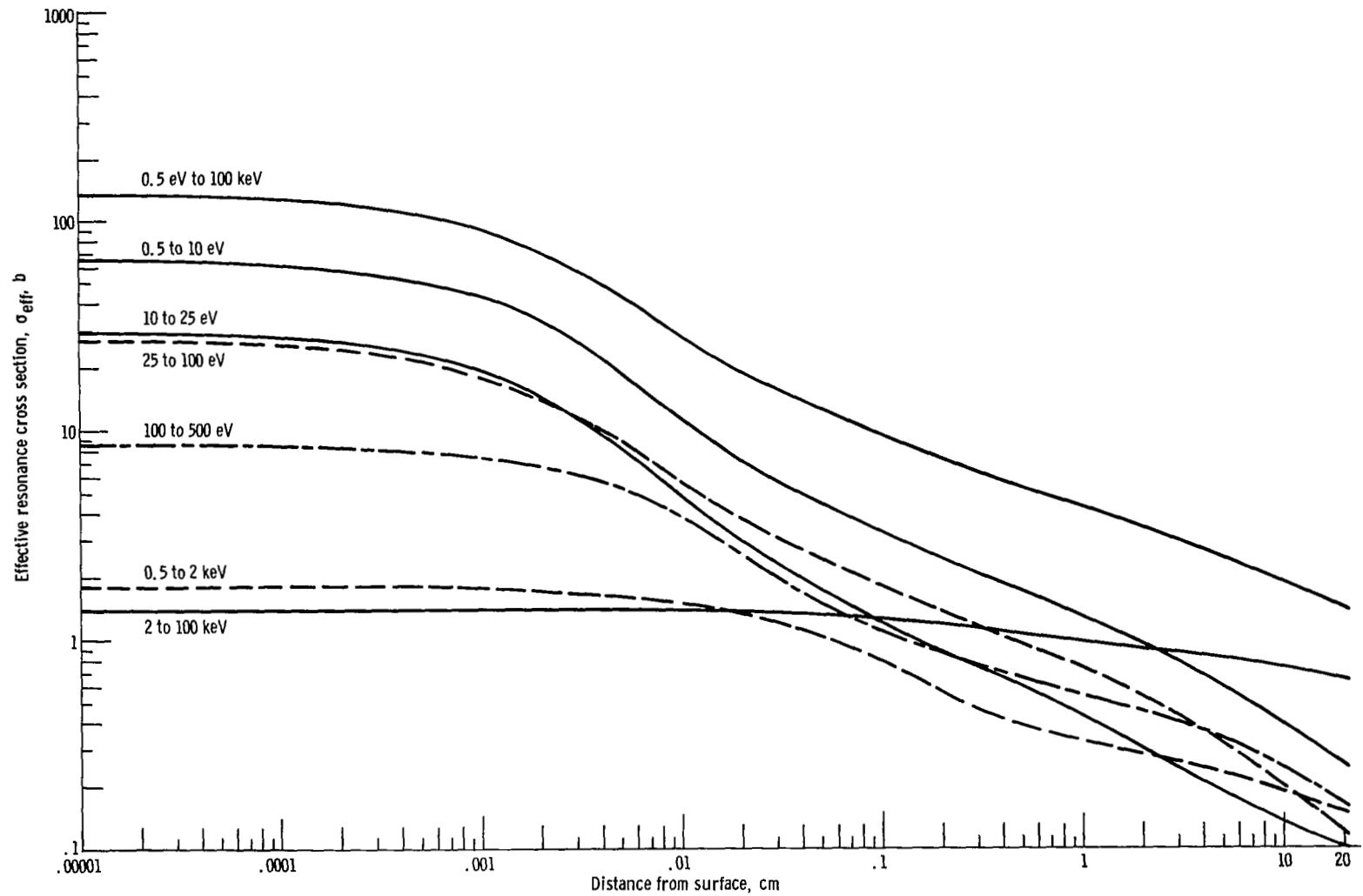


Figure 2. - Generalized group effective resonance cross sections for metallic uranium-238.

bulk of the absorber is caused by flux attenuation of the low cross sections in the overlap region between resonances.

Example. - As mentioned before, it is possible to estimate the distribution of spatial capture rate for thick slabs surrounded by moderators with different slowing down densities by independent consideration of group fluxes at the two surfaces of the slab. Such unsymmetrical spatial capture occurs in thick slabs of resonance absorbers considered for layered shields. The present generalized slab procedure may be applied directly to the results of broad group transport calculations and requires only the group fluxes at surfaces of absorber regions.

As an example, the method is applied to a 4-centimeter-thick uranium slab for neutrons in the group 0.5 to 10 eV. The left region flux ϕ_L is maintained as unity while the right region flux ϕ_R has values of $\phi_R = 0$ (corresponding to an outer shield layer of uranium), or $\phi_R = \phi_L/4$ (approximating the flux falloff in a shield layer surrounded by moderator), or $\phi_R = \phi_L$ (corresponding to a slab in a symmetrical flux). The distributions for these cases are shown in figure 3. The value of σ_{eff} at the left surface is one-half the dilute resonance integral of 134 barns for 0.5 to 10 eV neutrons. Also shown are the fractions of total capture up to several thicknesses. Relatively

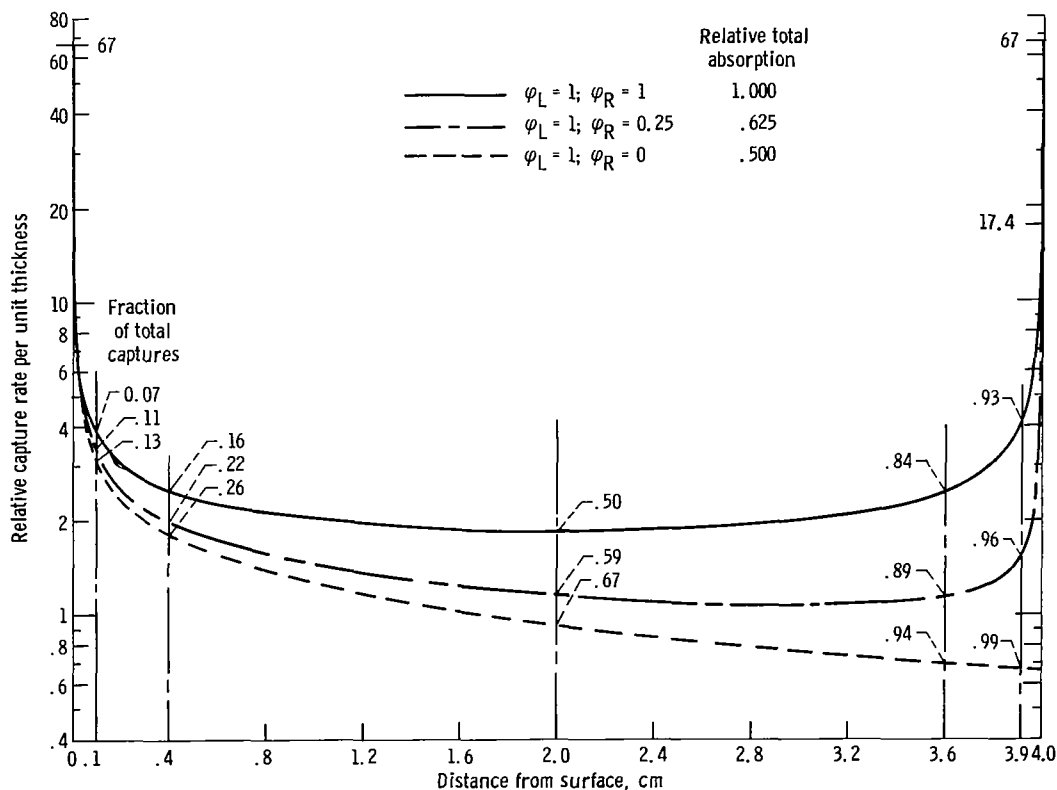


Figure 3. - Spatial distribution of captures per unit thickness in 4-centimeter-thick uranium slab for neutrons from 0.5 to 10 eV.

large capture fractions occur near the surfaces for slabs surrounded by moderator so that spatial capture gamma ray generation and escape from slabs are quite different from that of a transport calculation using a single group average capture cross section.

Specific comparisons of doses due to gamma rays generated in slabs by various multigroup treatment for symmetric fluxes were illustrated by Lahti (ref. 3). Additional examples for slabs in flux gradients will be presented in the next section of this paper. A comparison of the present analytical method with experiments for rods is presented in the final section.

APPLICATION TO LAYERED SHIELDS

Applications of the discrete ordinates method to the calculation of layered shields for reactor sources are being studied at Oak Ridge (ref. 11) and at NASA (refs. 12 and 13). At NASA (ref. 13), the weights of layered spherical shields for a fast spectrum nuclear reactor for space power have been calculated. The shield contains alternate layers of depleted uranium and natural lithium hydride and the thicknesses of the heavy layers were optimized (ref. 12) to meet a dose rate constraint of 2 millirem per hour at 20 meters from the shield.

The one-dimensional discrete ordinates transport program ANISN (ref. 14) was used with S_{16} quadrature and P_3 cross sections to obtain neutron flux distributions for 26 energy groups throughout the spherical reactor-shield configuration. This particular transport calculation is used to illustrate the differences in the spatial distributions within the depleted uranium layers that result from representing the resonance energy region by the multigroup method and by the present method. For this particular problem, group average cross sections for the resonance region were also generated by the code GAROL and are part of the set of cross sections precalculated and tabulated for the convenience of shield calculations by Lahti and Westfall (ref. 15).

The spherical geometry consisted of a reactor core, a pressure vessel, and a molybdenum reflector that is surrounded by a seven layered lithium hydride shield containing three layers of depleted uranium of thicknesses 6.12, 4.27, and 2.90 centimeters. The spherical layers are sufficiently large in radius so that they may be considered to be equivalent to infinite slabs.

The present method of estimating spatial capture distribution was applied to each layer of depleted uranium and for all neutron groups of the resonance region. It is noted that although the group GAROL average cross sections that represent the layered regions in the transport calculations can conserve total capture rates for the uranium layers, they do not produce the correct spatial capture rates. By a detailed comparison of the multibroad group transport results for this spherical shield with spatial capture results

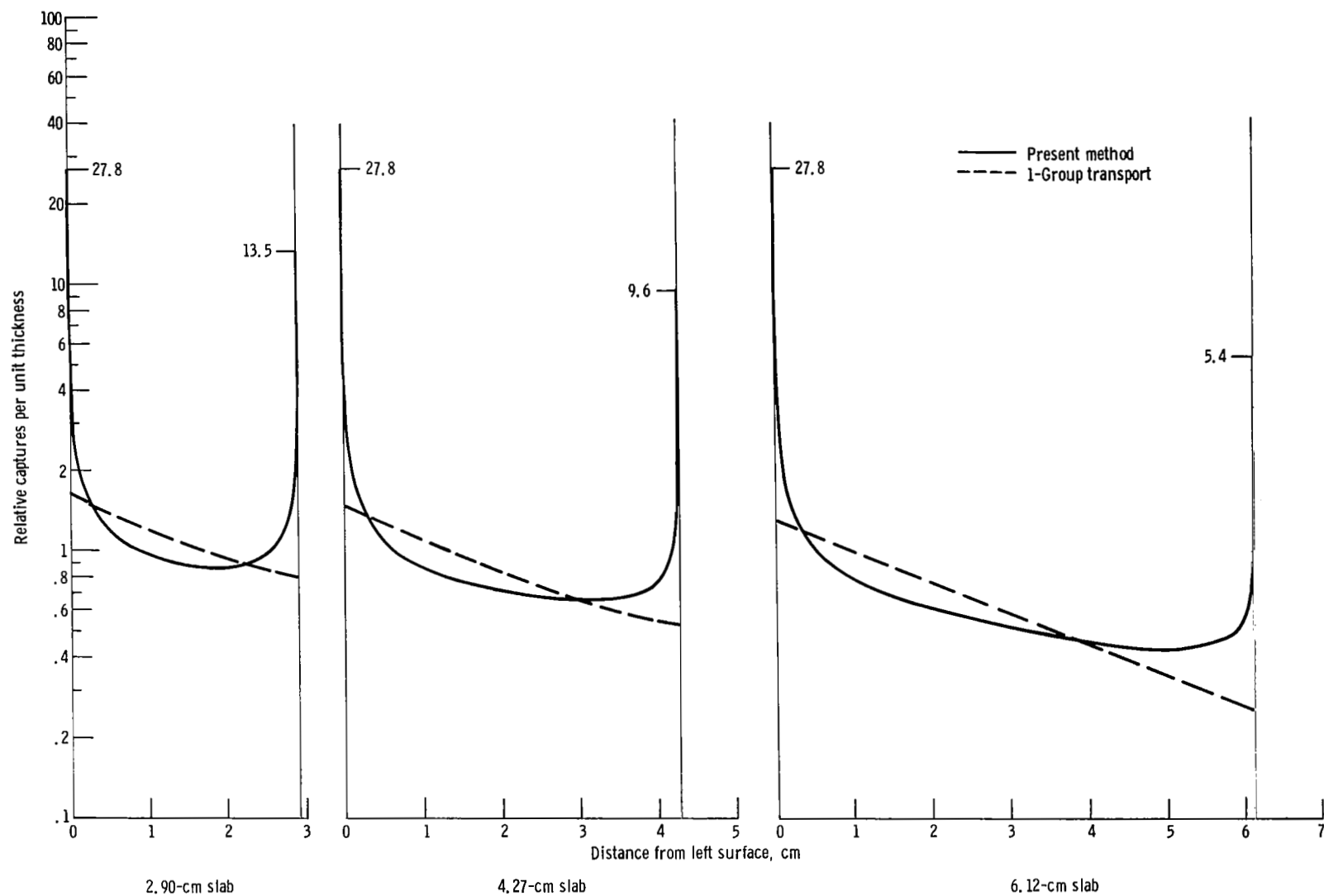


Figure 4. - Comparison of spatial capture rates in slabs of uranium-238 for neutrons in group 25 to 100 eV.

generated by applying the present method, it is possible to calculate the differences in the capture gamma ray escape fraction for the two spatial distributions. These calculations have been performed and the results for a few cases are illustrated.

Spatial capture differences. - A detailed comparison of the spatial capture rates in the three uranium layers are shown in figure 4 for neutrons in the group from 25 to 100 eV. The flux gradient across each uranium layer is primarily a function of its thickness and each thickness demonstrates a representative departure of the broad-group representation from a more accurate detailed spatial capture rate. In each case the broad one-group distribution shows essentially a single exponential fall-off of capture rate whereas the present method shows high surface region capture rates with rapid falloff and relatively flat capture in the bulk of the layers. Although the total captures have been made identical by normalization of both distributions, it is the large differences in capture rates at the outer surface regions of the layers that result in large differences in capture gamma ray escape.

For each spatial distribution, a group dose factor DF_i to a detector at the right surface of each slab was computed for the uranium layers. Each uranium slab of thickness t was taken to be approximated by an infinite plane gamma-ray source of thickness dx and DF_i was computed as:

$$DF_i(t) = \frac{\int_0^t S(x)_{\text{method}} E_1(b) dx}{\int_0^t S(x)_{1\text{-group}} E_1(b) dx} \quad (6)$$

where $S(x)$ are local values of captures per unit thickness, $E_1(b)$ is the exponential in-

tegral $\int_a^\infty (e^{-a}/a) da$, and b is the product of the mass absorption coefficient at

~ 2 MeV gamma-ray energy, uranium density, and distance x of source plane dx from the right surface of the uranium layers. These gamma-ray doses represent the uncollided components only. The dependence of the neutron capture gamma-ray spectrum on neutron energy may be important (ref. 16) in this calculation but has not been included in this example.

Each group dose factor was in turn weighted by the fraction of total resonance capture occurring in each group so as to arrive at a spectrally weighted dose factor for the

given slab layer thickness:

$$DF(t) = \frac{\int_i \left(\frac{\text{Captures}}{\text{Group}} \right)_i DF_i(t)}{\int_i \left(\frac{\text{Captures}}{\text{Group}} \right)_i} \quad (7)$$

The results of these calculations are presented in table III for the resonance region from 0.5 eV to 100 keV which in general encompassed about 85 percent of the total captures for the slab layers. The fraction of total captures and the dose factor are shown for six neutron groups in the resonance region from 0.5 eV to 100 keV for which the present method was formulated. The results for the three thicknesses of depleted uranium show the spectrally weighted dose factor to increase with layer thickness. This result is presented in figure 5 which shows the calculated dose factors to increase

TABLE III. - RELATIVE DOSES DUE TO CAPTURE GAMMA RAYS IN
SPHERICAL LAYERED SHIELDS OF DEPLETED URANIUM AND
LITHIUM HYDRIDE FROM SPATIAL DISTRIBUTIONS OF
CAPTURES CALCULATED BY PRESENT METHOD
AND BY A MULTIGROUP DISCRETE
ORDINATES METHOD

Neutron energy group	Thickness of depleted uranium layer, cm					
	2.90		4.27		6.12	
	Fraction of total captures	Dose factor	Fraction of total captures	Dose factor	Fraction of total captures	Dose factor
0.5 - 10 eV	0.156	1.32	0.143	1.48	0.156	1.81
10 - 25 eV	.079	1.36	.073	1.55	.080	1.85
25 - 100 eV	.125	1.33	.118	1.52	.135	1.76
100 to 500 eV	.132	1.31	.138	1.71	.138	1.94
0.5 - 2 keV	.237	1.41	.239	1.61	.237	2.07
2 - 100 keV	.105	1.28	.115	1.51	.114	1.42
0.5 eV - 100 keV	0.834	1.35	0.826	1.57	0.860	1.85

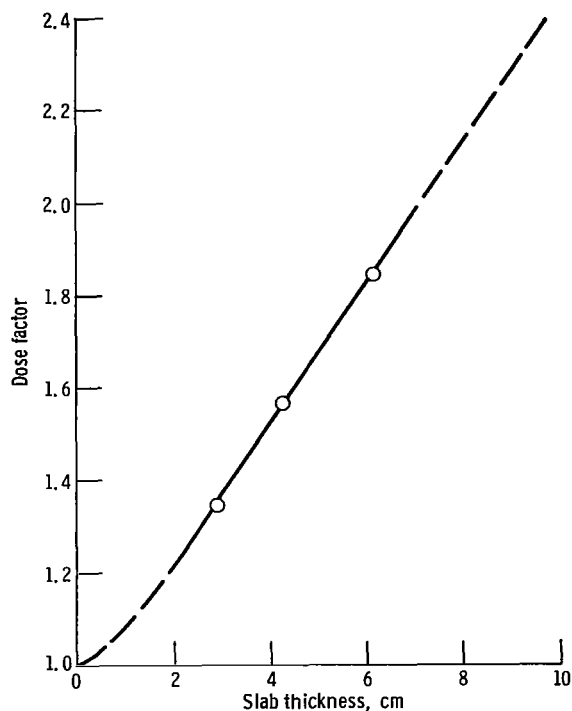


Figure 5. - Spectrum weighted dose factors for capture gamma rays in layered shields of depleted uranium and lithium hydride.

smoothly with layer thickness indicating a dose factor of 2.0 for a uranium layer thickness of 7 centimeters.

It is the large differences in calculated capture rates at the right surface regions that account for the large underestimate in capture gamma ray dose to a detector at the right surface of each uranium layer. The comparably large differences in calculated capture rates at the left surface regions do not affect the gamma dose at the right surface since these gamma rays are largely self-attenuated in traversing the uranium layer.

Because of the apparent generality of the present method, it is suggested that the method may be applied directly to the results of discrete ordinates multigroup calculations in order to estimate more accurately the spatial distributions of captures in thick slabs.

APPLICATION TO EXPERIMENTS WITH RODS

Some excellent experiments have been performed by Hellstrand (ref. 5) that measured the spatial distributions of resonance captures in rods of uranium. Because of the rapid depletion of resonance flux near the surface, it may be expected that the universal

functions $\sigma_{\text{eff}}(x)$ for slabs, shown in figure 2, will also apply for rods since the capture rate falls off rapidly at depths that are very much smaller than the radii of curvature of the surfaces.

In the Hellstrand experiments, the variations of epi-cadmium capture with depth in metallic uranium rods up to 5 centimeters in diameter were measured. The spatial distributions in rods were determined as part of a series of measurements of effective resonance integrals for uranium metal and oxide in various geometries. Resonance capture was measured by the activity of neptunium-239 induced in samples and the surface resonance flux was monitored by activation of thin gold foils. The results were evaluated in barns by using irradiated thin uranium samples as comparative standards using a dilute resonance integral of 280 barns for infinitely thin samples.

For these uranium rods, samples of metal at various depths were obtained by turning central sections on a lathe and collecting and counting the cuttings. The uncertainty in depth location of layers of measured rod activity near the surface due to machining was claimed to be ± 0.00012 centimeter. It should be noted that in this arrangement, samples of activated uranium collected near the surface of rods are exposed effectively only to the flux near the surface. On the other hand, induced activities are evaluated relative to infinitely thin foils of uranium which are activated by the unshielded flux on both surfaces. Therefore it should be expected that the activity induced near the surface of samples will approach a value of 140 barns or one-half of the uranium dilute resonance integral. Hellstrand designated these relative spatial activities as effective resonance cross sections which shall be seen to correspond to the values of capture rate per atom evaluated by the present method.

All cadmium covered rods were irradiated in the central channel of the Swedish heavy water reactor. In this connection it was pointed out by Hellstrand that all of his results do not include capture in the energy region from fission energy down to about 100 keV. This is so because the reactor location where samples were irradiated was removed from the reactor fuel and only a small part of the incident flux spectra extended above 100 keV. Therefore the calculated effective resonance integrals for the range 0.50 eV to 100 keV shown in table I apply directly to these experiments except for a convention observed by Hellstrand. This convention was to report all of his results as epi-cadmium non- $1/v$ effective integrals. Hellstrand assumed the $1/v$ part of the integral to be constant and equal to 1.1 barns corresponding to a cadmium cutoff of about 0.6 eV and a thermal absorption cross section of 2.75 barns. In order to compare the present integral and spatial calculations with Hellstrand, a comparable $1/v$ part of the integral was subtracted from the GAROL results.

A comparison of the calculated and measured epi-cadmium non- $1/v$ effective resonance integrals for uranium rods is given in table IV. Over the range measured the calculated GAROL results are in excellent agreement with Hellstrand's empirical fit to

TABLE IV. - COMPARISON OF CALCULATED
AND MEASURED EPI-CADMIUM NON-1/V
EFFECTIVE RESONANCE INTEGRALS
FOR URANIUM IN THE RANGE

0.50 eV - 100 keV

Slab thick- ness or rod radius, cm	Geometry parameter, $(S/M)^{1/2}$	Effective resonance integral, I_{eff} , b	
		GAROL	Hellstrand (a)
0.01	3.250	89.4	83.1
.05	1.454	39.7	38.7
.1	1.028	28.6	28.2
.5	.4595	14.2	14.2
1.0	.3250	10.8	10.8
2.0	.2300	8.3	8.5
5.0	.1454	5.8	6.4
7.0	.1230	5.1	5.8
10.0	.1028	4.4	5.4
15.0	.0840	3.6	4.9
20.0	.0727	3.2	4.6

^aFrom Hellstrand's fit to experiment:

$$I_{\text{eff}} = 2.81 + 24.7(S/M)^{1/2};$$

$$0.2 < (S/M)^{1/2} < 0.8.$$

his experiments; however for larger and smaller rods, the GAROL results deviate from this limited empiricism.

The question now arises of how to apply the values of $\sigma_{\text{eff}}(x)$ generated for the case of slabs to the case of infinitely long cylindrical rods of radius R placed in a moderator supporting a uniform slowing down flux. Although the variations of $\sigma_{\text{eff}}(x)$ with x are derived for slabs we assume that they also apply to a good approximation for rods of resonance absorber. This is based on the surface-to-mass correlation of I_{eff} for rods and slabs for which the same values of I_{eff} apply for equal values of surface-to-mass parameter (S/M) which generalizes results for many absorber geometries (see Dresner (ref. 7)).

Atoms near the surface of rods will have values of $\sigma_{\text{eff}}(x)$ of one-half the dilute resonance integral while atoms near the center of the rods will have values of $\sigma_{\text{eff}}(x)$ corresponding to the value of x equal to R ; intermediate values of $\sigma_{\text{eff}}(x)$ are assumed to correspond to the position along the diameter of the rod. With this assumption, the

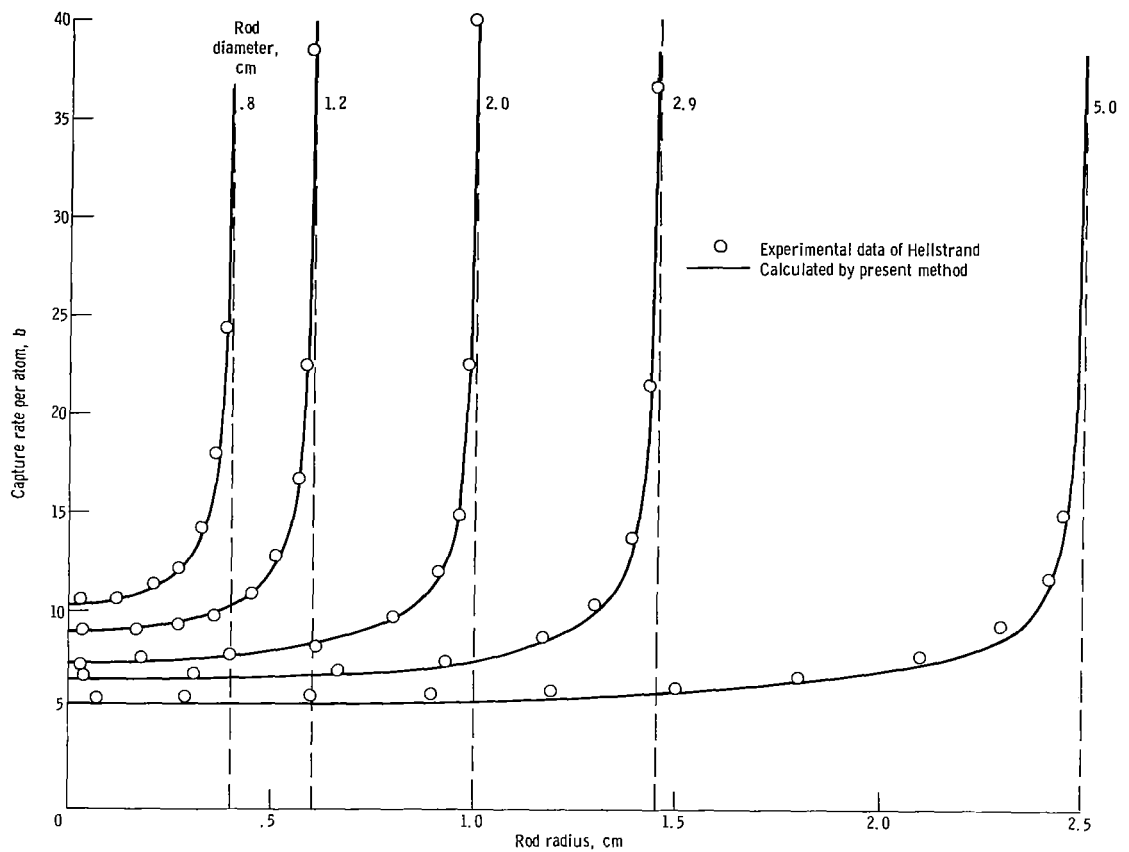


Figure 6. - Comparison of spatial distribution of captures calculated by present method with experimental data of Hellstrand for metallic rods of uranium-238.

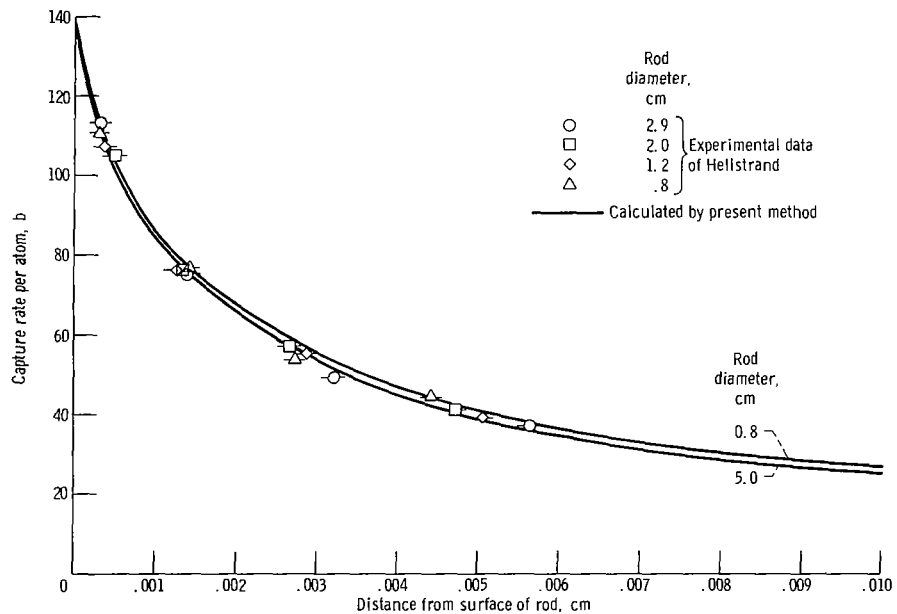


Figure 7. - Comparison of experimental and calculated spatial distribution of captures near surface of metallic rods of uranium-238.

spatial variation across the entire rod diameter is evaluated in the same manner as for slabs in which the distance from the rod surface x varies from 0 to $2R$.

The total captures per unit length of rod is given as

$$C = \int_0^R N\phi [\sigma_{\text{eff}}(x) + \sigma_{\text{eff}}(2R - x)] 2\pi r \, dr \quad (8)$$

The present method for estimating spatial distributions of captures has been applied to the rods measured by Hellstrand using the GAROL epi-cadmium non- $1/v$ effective resonance integrals from 0.50 eV to 100 keV to provide generalized values of σ_{eff} . These values of σ_{eff} are then used to calculate spatial capture distributions per atom that are directly comparable to the Hellstrand measurements. These comparisons are presented in figures 6 and 7. The calculations are absolute with no normalization and the agreement is particularly good over the bulk of the volume for all rods. In the small volume region near the surface the present method provides results in remarkable agreement with experiment. All the rods show the same rapid falloff of capture rate per atom from its value of one-half the dilute integral of 136 barns at the surface. Therefore, it may be concluded that the present method for estimating spatial distributions of captures in uranium slabs predicts experimental spatial distributions of captures in rods very well.

Lewis Research Center,
National Aeronautics and Space Administration,
Cleveland, Ohio, January 14, 1970,
124-09.

REFERENCES

1. Richtmyer, R. D.: Monte Carlo Study of Resonance Escape in Hexagonal Lattices. New York Univ. (AEC Rep. NYO-6479), 1955.
2. Kushneriuk, S. A.: Distribution of Resonant Neutron Capture in a Natural Uranium Rod - Application to NRX Rod 683. J. Nucl. Energy, Pt. A - Reactor Sci., vol. 10, no. 3/4, Sept. 1959, pp. 133-140.
3. Lahti, Gerald P.: Resonance Neutron Capture in a Thick Slab of Depleted Uranium. Trans. Am. Nucl. Soc., vol. 12, no. 1, June 1969, pp. 389-390.

4. Stevens, C. A.; and Smith, C. V.: GAROL, A Computer Program for Evaluating Resonance Absorption Including Resonance Overlap. Rep. GA-6637, General Atomic Div., General Dynamics Corp., Aug. 24, 1965.
5. Hellstrand, Eric: Measurements of the Effective Resonance Integral in Uranium Metal and Oxide in Different Geometries. J. Appl. Phys., vol. 28, no. 12, Dec. 1957, pp. 1493-1502.
6. Weinberg, Alvin M.; and Wigner, Eugene P.: The Physical Theory of Neutron Chain Reactors. Univ. Chicago Press, 1958, pp. 656-695.
7. Dresner, Lawrence: Resonance Absorption in Nuclear Reactors. Pergamon Press, 1960.
8. Nordheim, L. W.: A New Calculation of Resonance Integrals. Nucl. Sci. Eng., vol. 12, no. 4, Apr. 1962, pp. 457-463.
9. Kuncir, G. F.: A Program for the Calculation of Resonance Integrals. Rep. GA-2525, General Atomic Div., General Dynamics Corp., Aug. 28, 1961.
10. Stehn, John R.; et al.: Neutron Cross Sections. Vol. III. Z-88 to 98. Rep. BNL-325, 2nd ed., Suppl. 2, vol. 3, Brookhaven National Lab., Feb. 1965.
11. Mynatt, F. R.; et al.: The Discrete Ordinates Method - Shielding Applications. Neutron Physics Division Annual Progress Report for Period Ending May 31, 1967. Rep. ORNL-4134, Oak Ridge National Lab., Aug. 1967, pp. 50-56.
12. Lahti, Gerald P.: OPEX-II, A Radiation Shield Optimization Code. NASA TM X-1769, 1969.
13. Lahti, Gerald P.; and Herrmann, Paul F.: Comparison of Tungsten and Depleted Uranium in Minimum-Weight, Layered Shields for a Space Power Reactor. NASA TM X-1874, 1969.
14. Engle, Ward W., Jr.: A User's Manual for ANISN: A One-Dimensional Discrete Ordinates Transport Code with Anisotropic Scattering. Rep. K-1693, Union Carbide Corp., Mar. 20, 1967.
15. Lahti, G. P.; and Westfall, R. M.: Multigroup Resonance-Region Cross Sections for Tungsten and Depleted Uranium for Use in Shielding Calculations. NASA TM X-1909, 1969.
16. Yost, K. J.; and Solomito, M.: Sensitivity of Gamma-Ray Dose Calculations to the Energy Dependence of Gamma-Ray Production Cross Sections. Proceedings of Neutron Cross Sections and Technology Conference. D. T. Goldman, ed. Spec. Publ. 299, vol. 1, National Bureau of Standards, 1968, pp. 53-60.

NATIONAL AERONAUTICS AND SPACE ADMINISTRATION
WASHINGTON, D. C. 20546
OFFICIAL BUSINESS

FIRST CLASS MAIL



POSTAGE AND FEES PAID
NATIONAL AERONAUTICS A
SPACE ADMINISTRATION

08U 001 47 51 3DS 70103 00903
AIR FORCE WEAPONS LABORATORY /WLOL/
KIRTLAND AFB, NEW MEXICO 87117

ATT E. LOU BOWMAN, CHIEF, TECH. LIBRARY

POSTMASTER: If Undeliverable (Section 15
Postal Manual) Do Not Retu

"The aeronautical and space activities of the United States shall be conducted so as to contribute . . . to the expansion of human knowledge of phenomena in the atmosphere and space. The Administration shall provide for the widest practicable and appropriate dissemination of information concerning its activities and the results thereof."

— NATIONAL AERONAUTICS AND SPACE ACT OF 1958

NASA SCIENTIFIC AND TECHNICAL PUBLICATIONS

TECHNICAL REPORTS: Scientific and technical information considered important, complete, and a lasting contribution to existing knowledge.

TECHNICAL NOTES: Information less broad in scope but nevertheless of importance as a contribution to existing knowledge.

TECHNICAL MEMORANDUMS: Information receiving limited distribution because of preliminary data, security classification, or other reasons.

CONTRACTOR REPORTS: Scientific and technical information generated under a NASA contract or grant and considered an important contribution to existing knowledge.

TECHNICAL TRANSLATIONS: Information published in a foreign language considered to merit NASA distribution in English.

SPECIAL PUBLICATIONS: Information derived from or of value to NASA activities. Publications include conference proceedings, monographs, data compilations, handbooks, sourcebooks, and special bibliographies.

TECHNOLOGY UTILIZATION PUBLICATIONS: Information on technology used by NASA that may be of particular interest in commercial and other non-aerospace applications. Publications include Tech Briefs, Technology Utilization Reports and Notes, and Technology Surveys.

Details on the availability of these publications may be obtained from:

SCIENTIFIC AND TECHNICAL INFORMATION DIVISION
NATIONAL AERONAUTICS AND SPACE ADMINISTRATION
Washington, D.C. 20546